Submicron optical waveguides and microring resonators fabricated by selective oxidation of tantalum

Payam Rabiei,[1,*] Jichi Ma,[1] Saeed Khan,[1,2] Jeff Chiles,[1] and Sasan Fathpour[1,2]

[1]*CREOL, The College of Optics and Photonics, University of Central Florida, USA*
[2]*Department of Electrical and Computer Engineering, University of Central Florida, Bldg. 53, 4000 Central Florida Blvd., Orlando, FL 32816, USA*
[*]*pr@partow-tech.com*

Abstract: Submicron tantalum pentoxide ridge and channel optical waveguides and microring resonators are demonstrated on silicon substrates by selective oxidation of the refractory metal, tantalum. The novel method eliminates the surface roughness problem normally introduced during dry etching of waveguide sidewalls and also simplifies fabrication of directional couplers. It is shown that the measured propagation loss is independent of the waveguide structure and thereby limited by the material loss of tantalum pentoxide in waveguides core regions. The achieved microring resonators have cross-sectional dimensions of ~600 nm × ~500 nm, diameters as small as 80 µm with a quality, Q, factor of 4.5×10^4, and a finesse of 120.

©2013 Optical Society of America

OCIS codes: (130.0130) Integrated optics; (230.4000) Microstructure fabrication; (230.5750) Resonators; (230.7370) Waveguides.

References and links

1. E. A. J. Marcatili, "Dielectric rectangular waveguide and directional coupler for integrated optics," Bell Syst. Tech. J., 2071–2102 (1969).
2. E. A. J. Marcatili, "Bends in optical dielectric guides," Bell Syst. Tech. J., 2103–2132 (1969).
3. D. Marcuse, "Mode conversion caused by surface imperfections of a dielectric slab waveguide," Bell Syst. Tech. J., 3187–3215 (1969).
4. B. E. Little, S. T. Chu, H. A. Haus, J. Foresi, and J.-P. Laine, "Microring resonator channel dropping filters," J. Lightwave Technol. **15**(6), 998–1005 (1997).
5. D. Rafizadeh, J. P. Zhang, S. C. Hagness, A. Taflove, K. A. Stair, S. T. Ho, and R. C. Tiberio, "Waveguide-coupled AlGaAs / GaAs microcavity ring and disk resonators with high f inesse and 21.6-nm f ree spectral range," Opt. Lett. **22**(16), 1244–1246 (1997).
6. P. Rabiei, W. H. Steier, C. Zhang, and L. R. Dalton, "Polymer micro-ring filters and modulators," J. Lightwave Technol. **20**(11), 1968–1975 (2002).
7. B. Jalali and S. Fathpour, "Silicon Photonics," J. Lightwave Technol. **24**(12), 1400–1415 (2006).
8. P. Rabiei, "Calculation of losses in micro-ring resonators with arbitrary refractive index or shape profile and its applications," J. Lightwave Technol. **23**(3), 1295–1301 (2005).
9. D. K. Armani, T. J. Kippenberg, S. M. Spillane, and K. J. Vahala, "Ultra-high-Q toroid microcavity on a chip," Nature **421**(6926), 925–928 (2003).
10. K. K. Lee, D. R. Lim, L. C. Kimerling, J. Shin, and F. Cerrina, "Fabrication of ultralow-loss Si/SiO$_2$ waveguides by roughness reduction," Opt. Lett. **26**(23), 1888–1890 (2001).
11. S. Fathpour, K. M. Tsia, and B. Jalali, "Two-photon photovoltaic effect in silicon," IEEE J. Quantum Electron. **43**(12), 1211–1217 (2007).
12. D. Duchesne, M. Ferrera, L. Razzari, R. Morandotti, M. Peccianti, B. E. Little, S. T. Chu, and D. J. Moss, "High performance, low-loss nonlinear integrated glass waveguides," PIERS Online **6**(3), 283–286 (2010).
13. B. J. Eggleton, B. Luther-Davies, and K. Richardson, "Chalcogenide photonics," Nat. Photonics **5**, 141–148 (2011).
14. R. Y. Chen, M. D. Charlton, and P. G. Lagoudakis, "Chi 3 dispersion in planar tantalum pentoxide waveguides in the telecommunications window," Opt. Lett. **34**(7), 1135–1137 (2009).
15. C.-Y. Tai, J. S. Wilkinson, N. M. B. Perney, M. Netti, F. Cattaneo, C. E. Finlayson, and J. J. Baumberg, "Determination of nonlinear refractive index in a Ta$_2$O$_5$ rib waveguide using self-phase modulation," Opt. Express **12**(21), 5110–5116 (2004).
16. Y. C. Cheng and W. D. Festwood, "Losses in tantalum pentoxide waveguides," J. Electron. Mater. **3**(1), 37–50 (1974).

17. H. Takahashi, S. Suzuki, and I. Nishi, "Wavelength multiplexer based on SiO$_2$-Ta$_2$O$_5$ arrayed-waveguide grating," J. Lightwave Technol. **12**(6), 989–995 (1994).
18. B. Unal, C. Y. Tai, D. P. Shepherd, J. S. Wilkinson, N. M. B. Perney, M. C. Netti, and G. J. Parker, "Nd:Ta$_2$O$_5$ rib waveguide lasers," Appl. Phys. Lett. **86**(2), 021110 (2005).
19. C. A. Steidel and D. Gerstenberg, "Thermal oxidation of sputtered Tantalum thin films between 100° and 525°C," J. Appl. Phys. **40**(9), 3828–3835 (1969).
20. H. F. Winters and E. Kay, "Gas incorporation into sputtered films," J. Appl. Phys. **38**(10), 3928–3934 (1967).

1. Introduction

Integrated optical devices, based on microfabrication techniques, have been pursued for over four decades [1–3]. High-index-contrast waveguides, on a range of material systems [4–7], have been employed for achieving ultracompact and novel integrated photonic devices such as microring resonators and efficient nonlinear optical devices. Wide transparency range, low insertion loss and high nonlinear optical coefficients are important factors for an integrated optical platform.

Generally, integrated optical device technologies have been suffering from two major problems. First, etching processes that are typically used to define the waveguide ridges introduce sidewall roughness, from which guided light is scattered out of waveguides and the propagation loss can be significantly increased [8]. Second, achieving directional couplers, which are needed as part of many devices, require submicron gaps between waveguides. Achieving this is either very difficult or very expensive in practice. These problems have not been fully addressed and hence integrated optical devices with costs comparable to inexpensive electronic devices have been elusive to date.

Recently, some techniques have been introduced in order to eliminate surface roughness. For example, microresonators fabricated by selective reflow of patterned silica have shown ultrahigh quality factors, Q [9]. These resonators, however, are made in silica with air cladding which is not suitable for most practical applications. It has also been demonstrated that thermal oxidation of the dry-etched silicon ridge or channel waveguides smoothens the sidewalls and reduces the roughness loss [10]. Meanwhile, for many applications, e.g., biosensing, nonlinear optics and quantum optics, it is needed to achieve devices that can operate in the visible spectrum. Silicon, however, has a limited transparency range that hinders its application for the visible spectrum. Furthermore, it suffers from two-photon absorption and associated free-carrier scattering which degrade the performance of nonlinear optical processes in silicon photonics [11]. Compact integrated photonic platforms that operate from visible to infrared wavelengths and can be yet fabricated on silicon substrates are highly desired.

Among other materials [12,13], oxides of refractory metals, such as tantalum (Ta), are perfect candidates for this purpose. They are transparent in visible and infrared wavelengths and have high refractive indices of ~2.2, which allows fabrication of high-index contrast waveguides on low-index cladding layers, such as silicon dioxide (SiO$_2$), on silicon substrates. Tantalum pentoxide (Ta$_2$O$_5$) possesses large third order nonlinear optical coefficients and high optical damage threshold [14,15]. Ta$_2$O$_5$ waveguides have been demonstrated in the past by using standard lithography and reactive ion etching methods [16–18]. Cheng *et al*. [16] demonstrated such waveguides in 1970s. Arrayed waveguide grating devices were demonstrated using tantalum Ta$_2$O$_5$ in 1990s [17]. More recently, rare earth doped Ta$_2$O$_5$ waveguides have been demonstrated by sputtering from doped Ta$_2$O$_5$ targets and reactive ion etching methods [18].

A very unique property of tantalum is the ability to be oxidized at relatively low temperatures [19]. In this paper, we exploit this unique property in order to achieve low-loss submicron waveguides. For the first time, a novel method for fabrication of high-contrast submicron waveguides based on selective oxidation of a refractory metal (SORM) is introduced. The method eliminates the sidewall surface roughness scattering and at the same time achieves submicron gaps between waveguides without the need of expensive lithographic and etching methods and allows demonstration of high-contrast and low-loss waveguides on silicon substrates. Tantalum pentoxide microring resonators are demonstrated

here for the first time in the telecommunication wavelengths. We believe that the demonstrated fabrication method allows low-cost and reliable integrated optical devices to be realized for the mentioned host of applications.

2. Fabrication technique

The SORM method proposed here is based on selective oxidation of Ta to form a waveguide on a silicon substrate. Figure 1 shows the fabrication procedure. Tantalum is first deposited using a sputtering tool on a silicon substrate with a SiO_2 buffer layer grown by thermal oxidation. Next, a SiO_2 mask layer is deposited on the tantalum surface using a plasma-enhanced chemical vapor deposition (PECVD) chamber and then patterned by electron-beam lithography to open a narrow slot in the SiO_2 mask layer. It is noted that e-beam lithography is used due to its availability. However, the proposed fabrication method does not necessarily need very small feature sizes made by e-beam lithography. The sample is then placed in a furnace with oxygen flow at 520°C to selectively convert Ta into Ta_2O_5 in the exposed regions of the SiO_2 mask layer. In the subsequent steps, the SiO_2 layer is removed and the remaining Ta layer is etched away and a channel waveguide is hence achieved. A top cladding layer of SiO_2 layer is finally deposited on the channel waveguides.
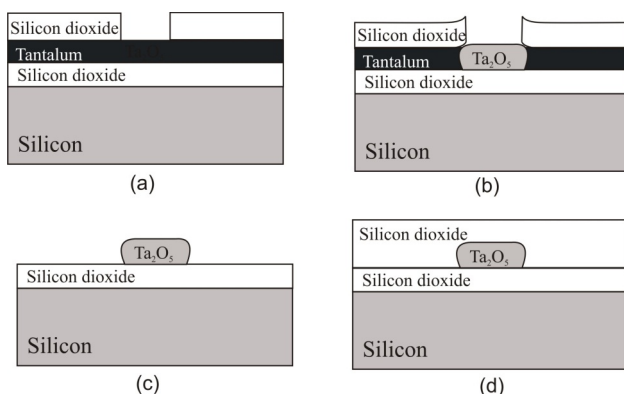

Fig. 1. The processing steps of the proposed SORM waveguide fabrication technique.

During the oxidation process the oxygen diffuses into the tantalum layer underneath the SiO_2 mask layer as shown in Fig. 2(b). It is well-known that the diffusion process eliminates the sidewall roughness that exists on the mask layer and allows ultra-smooth surfaces to be achieved [10]. The oxidation process also causes inflation of the tantalum layer. The thickness of the resulting Ta_2O_5 layer is approximately twice the original tantalum layer. Also, it is noted that since Ta can be etched highly selectively compared to Ta_2O_5, the final tantalum etching step does not introduce any roughness in the remaining Ta_2O_5 waveguide layer.

Ridge waveguides can also be fabricated by a slight modification in the above process. That is, a Ta layer deposited on the SiO_2 buffer layer is fully oxidized first to form a Ta_2O_5 slab layer. Then, a second layer of Ta is deposited on the Ta_2O_5 slab and selectively oxidized, similar to the steps of Fig. 1, to form a ridge waveguide.

Figure 2 shows scanning electron microscope (SEM) images of cleaved facets of the fabricated ridge and channel waveguides. In the ridge waveguide case (Fig. 2(a)), the waveguide is formed into a trapezoidal shape with a base of about 1 μm. In the channel waveguide case (Fig. 2(b)), however, the resulting waveguide is dome-shaped. It appears that the underlying layer (Ta_2O_5 and SiO_2 in Figs. 2(a) and 2(b), respectively) can profoundly
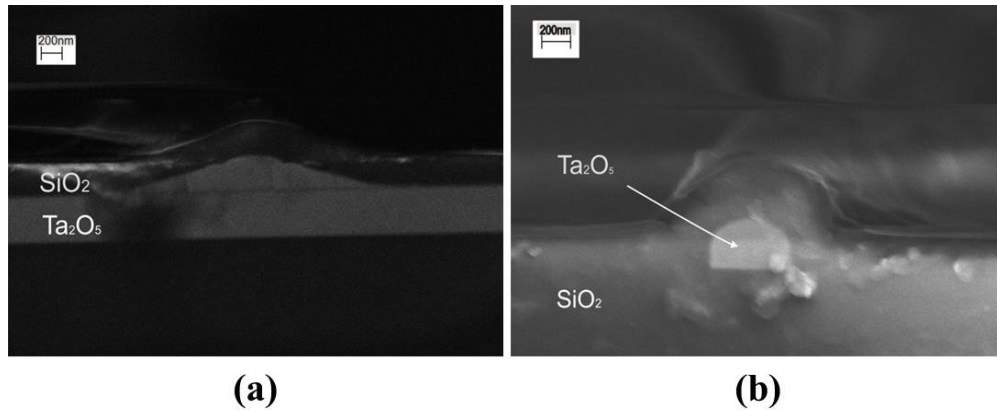
Fig. 2. The SEM cross-section images of the fabricated devices: (a) ridge and (b) channel waveguides.

influence the oxidation process and the shape of the resulting waveguide. The difference can be attributed to the much higher diffusion constant of oxygen in Ta_2O_5 than SiO_2.

Propagation losses of <10 dB/cm from such straight ridge waveguide, with different base widths ranging from 600 to 1200 nm, were measured using the Fabry-Perot (FP) technique for the ridge waveguides. Negligible sensitivity of FP fringes and transmitted power for waveguides with various widths suggests that the modest loss is not related to sidewall scattering. As follows, channel waveguides as well as ridge and channel microring resonators were fabricated to further investigate this.

In addition to eliminating the surface roughness problem, the explained novel fabrication method eliminates the need for expensive lithographic and etching tools needed for achieving submicron gaps in integrated optics. Generally, very precise gaps on the order of 100 nm are needed in order to achieve high coupling between high-index contrast waveguides and resonators. One advantage of the SORM fabrication technique is that such extremely narrow and precise waveguide gaps can be readily achieved with low-cost lithography and etching methods. In SORM, the gap width can be controlled accurately by the oxidation time, and its accuracy is less related to the lithographic and etching steps. In the following results, such small gaps on the order of 100 nm with a few nm of accuracy are reported.

In order to demonstrate all the claims for our new fabrication method, we have made micro-ring resonators fabricated using this technology. Figure 3 shows a microscope image of our fabricated microresonator device. As can be seen, a microresonator is coupled to two input and output waveguides. There is also two bends from input to output to study the effect of bending loss in the device in addition to scattering and material losses that will be obtained by measuring the resonators' Q, as discussed below.

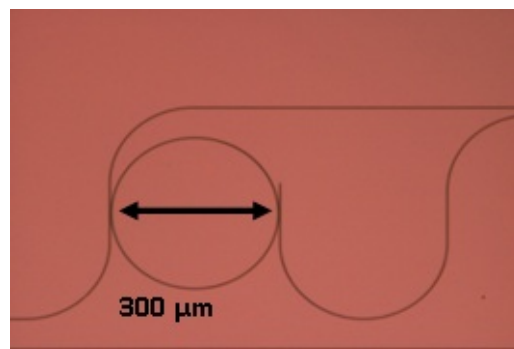Fig. 3. Microscope image of fabricated microring resonator with input and output coupled waveguides.

3. Characterization and discussion

The first device that was fabricated was a microresonator using ridge waveguides. Figure 2(a) shows the device cross-section. Devices with diameters ranging from 200 µm and larger were fabricated based on the calculation results that showed negligible bending loss. Figure 4(a) shows the measured transmission spectrum of a 300-µm diameter device for two different coupling strengths between the waveguides and the resonator (corresponding to 2.6 and 2.8 µm gaps on the mask) for the transverse electric (TE) mode at a center wavelength of 1550 nm. It is evident that single-mode resonances are experimentally observed. By increasing the coupling, the resonance peak width increases, as expected, and the device performs closer to the critical coupling point. Based on these measurements, the propagation loss of the waveguide and the coupling strength were extracted by curve fitting according to standard ring-resonator theories [6]. The extracted propagation loss is 9.5 dB/cm in a 300-µm diameter device, the estimated unloaded Q is ~4×10^4 and the unloaded finesse is 30. The coupling coefficient was calculated and an exponential decay as a function of linear gap was obtained, in agreement with the theory (see Fig. 4(b)).
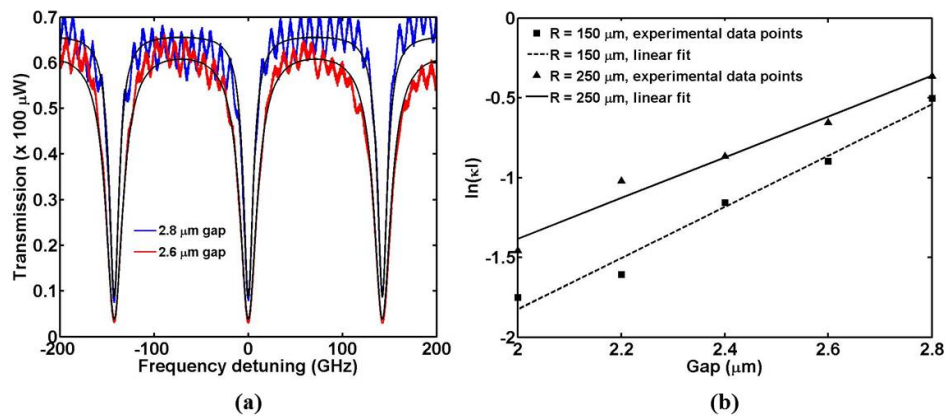

(a)   **(b)**

Fig. 4. (a) TE transmission spectrum of a device with 300-µm diameter and for two coupling strengths (colored lines) and the fitted spectra (black lines) around 1550 nm; (b) Measured and fitted coupling coefficient times length ($\kappa \times l$) as a function of the coupling gap for two different microring radii.

The input polarization was also changed to transverse magnetic (TM). The guided light, however, converted to the TE mode in the device. This can be explained by noting that the effective index of the TE and TM modes are very close to each other for this ridge structure. Hence, the TM mode can easily couple to the TE mode by small perturbations in the device. The TE-mode effective index is slightly larger, however, and the guided light will remain in this mode after conversion.

Next, the slab waveguide region was eliminated in the fabrication process (see Fig. 1), and channel waveguides and microresonators were demonstrated. Figure 2(b) shows a typical waveguide cross-section SEM image confirming a Ta_2O_5 core region with approximate dimensions of 500 nm × 600 nm, and with a shape qualitatively in agreement with the schematic of Fig. 1(d). Since the index contrast in these channel waveguides is larger than the discussed ridge waveguides, more compact ring-resonators can be attained. Microresonators with diameters ranging from 20 to 80 µm were fabricated based on calculation results that demonstrate negligible bending loss. Figure 5(a) shows the transmission spectrum of a device with 80 µm diameter both for TE and TM modes. The extracted unloaded Q for this device is equal to 4.5×10^4. The propagation loss, based on the measured Q, is 8.5 dB/cm for both TE and TM modes. Remarkably, the measured loss for this microresonator with a smaller channel cross-section is slightly lower than the ridge waveguides discussed before.

In order to experimentally confirm that the measured loss is not due to bending loss, we measured the transmission for smaller diameter devices. Figure 5(b) shows the TM-mode

transmission spectrum for a 40-μm diameter device. Since there are two bends between the input and output (see Fig. (3)) and since the bending loss is highly wavelength-dependent and not negligible in this case, there is a drop in the transmitted power as a function of wavelength and the resonance width is slightly increased too. However, no wavelength-dependent insertion loss is observed in the presented 80-μm diameter device and hence the bending loss is negligible in that device. Similar behavior is observed in the ridge waveguides (Fig. 4(a)).

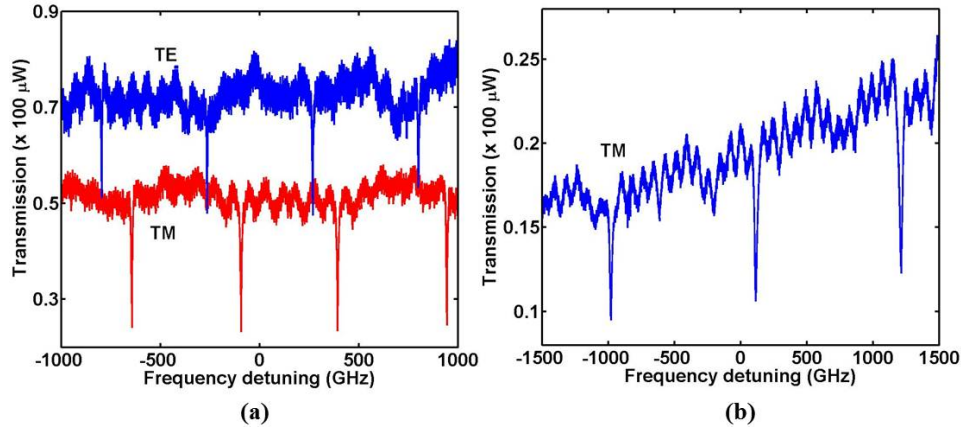Fig. 5. (a) Transmission spectrum of a channel-waveguide-based microresonator with 80 μm diameter for TE and TM modes around 1550 nm; (b) Transmission spectrum of a channel-waveguide-based microresonator with 40 μm diameter for TM modes around 1550 nm. The bending loss is considerable in this case.

Based on the presented results, it is evident that the propagation loss in all the fabricated devices is limited to about 8.5 to 9 dB/cm regardless of the waveguide structure (ridge versus channel) and ridge waveguide base width (600 nm to 1200 nm). Also, similar values of loss have also been previously reported for much wider tantalum pentoxide waveguides made by conventional fabrication methods [14]. The scattering loss is highly dependent on the dimensions of the device since the scattered light is proportional to the quadratic power of the electric field which is much larger for smaller devices. Since no change in the measured propagation loss for waveguides ranging from several microns to submicron dimensions is observed, it is clear that the loss can only be attributed to material absorption in the Ta_2O_5 core region and not to sidewall scattering or bending loss. The slight decrease in the loss for smaller devices can then be explained by slightly less confinement of the mode in the waveguide core.

The rather high material loss of Ta_2O_5, meanwhile, could be due impurities in the sputtered Ta metal deposition. It is known that gases like argon and nitrogen can be incorporated in sputtered metallic films [20]. Higher material quality may be possible if other deposition techniques are employed to form the Ta layer(s).

4. Conclusions

In conclusion, ring resonator devices were demonstrated for the first time in tantalum pentoxide waveguides on silicon substrate by using a novel fabrication method, named SORM. Propagation losses as low as 8.5 dB/cm were obtained in Ta_2O_5 submicron waveguides and it is evidenced that the loss is not related to scattering from the surface roughness or bending loss but rather attributed to material absorption in the core region. Submicron gaps needed for compact couplers were achieved based on the proposed fabrication method, which led to the demonstration of submicron Ta_2O_5 microring resonator, for the first time, with diameters as low as 80 μm with finesses as high as 120 and quality factors as high as 4.5×10^4. Further, research is needed in order to identify the cause of the material loss. It is expected that if the material loss is eliminated, ultrahigh-Q and ultralow loss devices can be made using the novel technique described in this paper.